Micropatterning of reagent-free, high energy crosslinked gelatin hydrogels for bioapplications

Benedikt Heyart[a], Astrid Weidt[b], Emilia Wisotzki[a], Mareike Zink[b] and S.G. Mayr[a,c,*]

[a] Leibniz Institute for Surface Modification (IOM), Permoser Str. 15, 04318 Leipzig, Germany

[b] Soft Matter Physics Division, Institute for Experimental Physics 1, University of Leipzig, Linnéstr. 5, 04103 Leipzig, Germany

[c] Division of Surface Physics, Department of Physics and Earth Sciences, University of Leipzig, Leipzig, Germany

*Corresponding author: Stefan.Mayr@iom-leipzig.de

Abstract

Hydrogels are crosslinked polymeric gels of great interest in the field of tissue engineering, particularly as biocompatible cell or drug carriers. Reagent-free electron irradiated gelatin is simple to manufacture, inexpensive and biocompatible. Here, the potential to micropattern gelatin hydrogel surfaces during electron irradiation crosslinking was demonstrated as a promising microfabrication technique to produce thermally-stable structures on highly relevant length scales for bioapplications. In the present work, grooves of 3.75 to 170 µm width and several hundred nanometers deep were transferred onto gelatin hydrogels during electron irradiation and characterized by 3D confocal microscopy after exposure to ambient and physiological conditions. The survival and influence of these microstructures on cellular growth was further characterized using NIH 3T3 fibroblasts. Topographical modifications produced surface structures on which the cultured fibroblasts attached and adjusted their cell morphology. This developed method allows for simple and effective structuring of gelatin and opens up new possibilities for irradiation crosslinked hydrogels in biomedical applications in which cell attachment and contact guidance are favored.

1. Introduction

Tissue engineering research is concerned with the restoration, maintenance and improvement of tissue functions ((Langer and Vacanti 1993; Ma 2004, 2005, 2008). The therapeutic approach often consists of the removal of patient cells, subsequent colonization of a carrier with biological cells and transplantation of the carrier into the patient (El-Sherbiny and Yacoub 2013). For example, cholecyst-derived scaffolds have been examined by Revi et al. as biomimetic skin grafts for medical application to patients with extensive burn wounds (Revi et al. 2016). Moreover, biomimetic grafts for vascular surgery that mimic native blood vessels are employed for patients which cannot be supplied which autologous blood vessels (Prasad Chennazhy and Krishnan 2005). Here, hydrogels are potentially suitable as graft materials and cell carriers for regenerating and repairing soft tissues. Specifically, gelatin is promising biomimetic material, as it stems from collagen and therefore exhibits similar properties to the extracellular matrix (ECM). Yet, with a sol-gel transition temperature below 37°C as well as decreasing mechanical stability and elasticity

as a result of swelling effects, the applicability of pure gelatin is limited. However, modifications and functionalization can increase the potential for applications in physiological environments (Sefton et al. 2012).

For usage as cellular substrates, hydrogel surfaces are often functionalized with proteins and polymers to improve and promote cell-surface interactions. Cells perceive and react to various biochemical and biophysical signals from the microenvironment (Teixeira et al. 2003). In the nano- and micrometer range, the ECM topography exhibits a variety of structures (Stevens 2005). The interaction of cells with the topography is mediated by the contact guidance phenomenon (Rørth 2011) which influences cellular processes such as adhesion, morphology, differentiation and migration of cells (Dent and Gertler 2003; Wolf 2003; Haga et al. 2005; Friedl 2004; Luca et al. 2015). Grooves of a few µm in size are the most widely studied surface structures of hard materials. Typically, cultured cells align with the major axis along the grooves. Narrower and deeper grooves generally support the development of increasingly elongated cell morphologies (Nikkhah et al. 2012).

Microfabrication is a widely used method to achieve such small structures on substrates. Photolithography was among one of the first fabrication methods applied to cell morphology studies, used to generate rigid structures in inorganic materials such as silicon and silicon dioxide (Chou et al. 1995; Dunn and Brown 1986; Wood 1988; Wójciak-Stothard 1995; Wójciak-Stothard et al. 1995; Meyle et al. 1995). However, due to rigidness and resistance to degradation, these materials are unsuitable for biomedical applications in soft tissues. In recent years, novel approaches have used soft lithography techniques to pattern elastomeric materials. A master template is typically fabricated and used to mold, imprint or emboss structures onto soft materials (Weibel et al. 2007). The mechanically integrity of the patterned material is therefore of great importance for the structural stability (Billiet et al. 2012). Resultantly, the polymeric materials must exhibit a specific degree of rigidity, leading to the wide use of materials such as polydimethysiloxane (PDMS; Uttayarat et al. 2005; Biela et al. 2009; den Braber et al. 1996b; den Braber et al. 1998). Alternatively, the polymers can be crosslinked during the molding process to increase stability, however it can be challenging to obtain homogenous crosslinking using chemical methods. Hyaluronic acid (Khademhosseini et al. 2006; Yeh et al. 2006) and chitosan-

based (Fukuda et al. 2006) hydrogels have been successfully micromolded and crosslinked by UV irradiation. However, this method requires photocrosslinkable materials and is limited by the depth of penetration of the UV radiation. Other hydrogels such as alginate and fibrin require the addition of gelling agents such as divalent cations, complicating the preparation of a controlled shape and size (Khademhosseini and Langer 2007). Reagent-free electron irradiation of specific polymers, such as gelatin, is a physical crosslinking method used to produce covalent crosslinks, but has not been examined in combination with the micromolding process thus far. In addition to a large, homogeneous penetration depth profile, the lack of chemical reagents required means that toxic residues are not left in the material, in contrast to crosslinking with chemical agents. This crosslinking technique can be used to significantly increase the mechanical strength, heat stability and swelling stability of gelatin hydrogels. For 10 wt% gelatin, the storage modulus increased from 7 kPa to 11 kPa after irradiation with 40 kGy (Wisotzki et al. 2014). Furthermore, doses on this order of magnitude result in sterilization of the samples and have exhibited good biocompatibility with NIH 3T3 fibroblasts (Wisotzki et al. 2016).

This present work establishes a method of transferring µm-sized grooves onto gelatin hydrogels by micromolding. Since low mechanical strength hinders such microfabrication techniques (Billiet et al. 2012), crosslinking by electron irradiation was used to tune the mechanical properties and stabilize the patterned microstructures in ambient and physiological conditions. Through cell experiments employing NIH 3T3 fibroblasts, the generated topography demonstrated significant influence over the adhesion and morphology of seeded cells.

2. Materials and methods

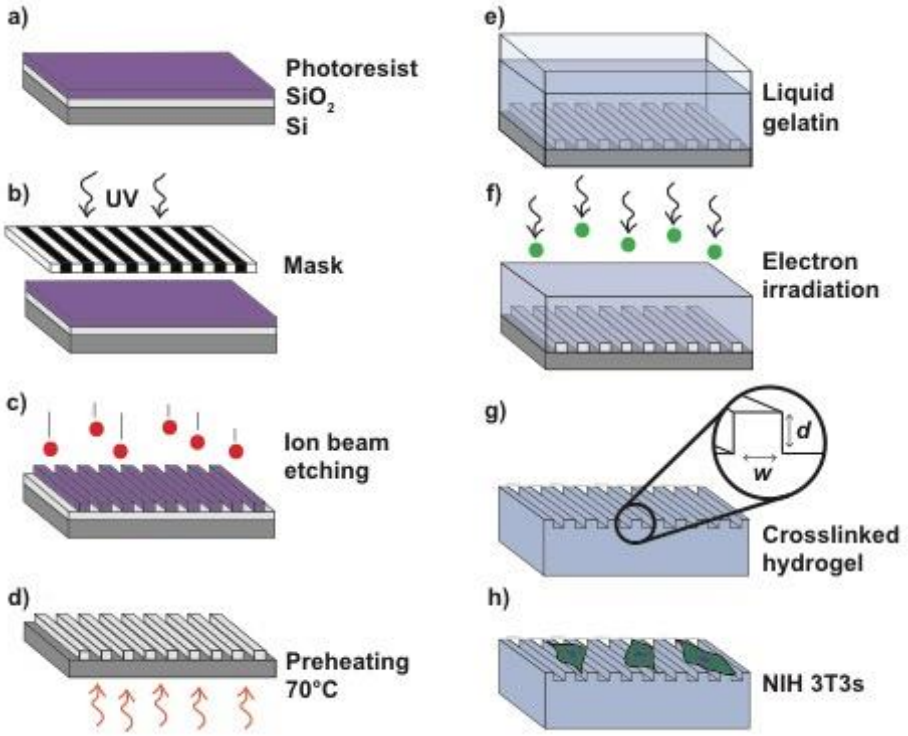

Figure 1 A summary of the fabrication steps used to synthesize the templates (left) and micropatterned gelatin hydrogels (right). In subfigure g), the enlarged diagram shows how the width (*w*) and depth (*d*) profiles were defined for the grooved structures.

2.1. Template fabrication

Templates were manufactured on silicon wafers using photolithography, as summarized by steps a) to d) in Figure 1. Silicon wafers had a natural silicon dioxide layer, which was coated with positive AZ MiR 701 photoresist (Micro Chemicals GmbH, Ulm, Germany) and developed with AZ 726 MIF (Micro Chemicals GmbH, Ulm, Germany). Two different templates were fabricated with ion beam etching. The first template consisted of 3.75 µm-wide grooves of 800 nm depth, periodically repeating with 3.75 µm spaces in between. The second template had 500 nm deep grooves, with four different repeating widths of 17 µm, 50 µm, 96 µm and 170 µm. Resulting templates were 2 cm by 2 cm.

After fabrication, templates were cleaned using the RCA cleaning process with two cleaning solutions (first solution: ammonium hydroxide (30 %), hydrogen peroxide (30 %) and deionized water in the ratio 1:1:5; second solution: hydrochloric acid (37 %), hydrogen peroxide (30 %) and

deionized water in the ratio 1:1:6). Wafers were ultrasonicated in each solution for 30 to 45 min. In between the cleaning steps, templates were rinsed for 1 to 2 min with deionized water. Samples were dried by spin-coating at 4000 rev/min and subsequently heated to 115 °C for 2 to 5 min on a hot plate.

2.2. Hydrogel synthesis

Type A porcine skin gelatin (Bloom 300, Sigma Aldrich, G2500) was used to synthesize 10 wt% hydrogels. Gelatin powder was swollen in deionized water for approximately 1 h before heating to 60 °C until complete dissolution. The molding process is illustrated by steps e) to h) in Figure 1. The structured templates were placed at the bottom of 2 cm by 2 cm silicone molds on top of aluminum plates for stabilization. Templates were preheated to 70 °C to improve the flow of gelatin into the grooves. Subsequently 0.8 mL of gelatin solution was pipetted into the templates. The molds were sealed and stored for 24 h at 10 °C. Afterwards, samples were transferred to air-tight plastic bags with the template still attached, in preparation for irradiation. Samples were irradiated with a 10 MeV linear accelerator (Mevex, Ontario, Canada) on a moving stage with a 180 Hz repetition rate and 8 µs electron pulse length, using a scanning horn (width 620 mm, scanning frequency 3 Hz). A predetermined dose of 40 kGy was used, measured by a graphite dosimeter with 5 % uncertainty. Prior to surface analysis and cell experiments, the irradiated gelatin was gently detached from the template so that the template pattern remained inverted on the gelatin surface.

To determine the influence of electron irradiation on the pattern transfer, unirradiated and 40 kGy irradiated gelatin hydrogels were prepared from each template. Irradiated samples were analyzed after 1 d and 5 d exposure to physiological conditions, i.e. at 37 °C in Hank's Balanced Salt Solution (HBSS; Sigma Aldrich, H8264) with 1 % penicillin-streptomycin (A & E Scientific (PAA), P11-010) to protect against bacterial contamination. Before surface analysis, residual HBSS was removed from the hydrogel surface with a N_2 stream.

For cell tests, samples with the 3.75 µm grooved template were used. For comparison, unstructured samples were prepared in direct contact with smooth aluminum plates. The detached gelatin films were washed with phosphate-buffered saline (PBS). Gels were punched to

fit tightly into 12 well plates for cell culture. Before seeding cells on the structured surfaces, the gelatin hydrogels were incubated overnight at 37 °C.

2.3. Surface analysis

The patterned hydrogel and template surfaces were analyzed with a 3D confocal microscope µsurf explorer (NanoFocus AG, Oberhausen, Germany) using µsoft metrology software version 7.4.0. Samples were placed with the structured side upwards and measured at 20x magnification. Since the maximal measurement range was 800 µm by 800 µm, several areas were analyzed on each sample for statistical purposes. For visual comparison, 3D maps were collected from each sample. Using the µsoft software, the depth and width of the grooves were determined from the profiles of the gelatin surfaces, as illustrated in subfigure 7) of Figure 1. According to the analysis software, the side walls of the trenches were not parallel but tapered. Hence, the values for the widths were measured at half height.

For easier comparison with the template profiles, the resulting data from the hydrogels was inverted and smoothed by an 8^{th} degree polynomial. For the silicon templates, only the width of the grooves could be determined by this optical technique because of limitations caused by the transparency of the silicon dioxide layer. Therefore, the groove depths were characterized by atomic force microscopy (Veeco Dimension Icon, Veeco Instruments Inc., New York, USA).

2.4. NIH 3T3 cell tests

NIH 3T3 fibroblast cells (ATCC, CRL-1658) were cultured at 37 °C and 5 % CO2 atmosphere in Dulbecco's Modified Eagle's Medium (DMEM, PAA Laboratories GmbH, E15-810) supplemented with 10 % calf serum (PAA, B15-004) and 1 % penicillin-streptomycin (A & E Scientific (PAA), P11-010). The culture medium was renewed every 2 to 3 days and fibroblasts were subcultured at max. 80 % confluence. For the gelatin experiments, the fibroblasts were detached by adding 0.25 % Trypsin-EDTA (PAA, L11-004) and seeded in the wells onto the prepared hydrogels. Cultivation was carried out for 1 day (4000 cells/cm^2) and 4 days (400 cells/cm^2).

For analysis of the cell morphology 1 day and 4 days after seeding, the fibroblasts were fixed with 4 % paraformaldehyde (Sigma-Aldrich, P6148) for 15 to 20 min. Subsequently, cells were washed twice with PBS. Cells were permeabilized with 0.1 % Triton X-100 (v/v, Sigma-Aldrich, X100) for 5 min, then washed twice with PBS. The actin filaments were stained using a solution of 1.5 µl/ml

rhodamine phalloidin (Sigma-Aldrich, P1951) in PBS for 30 min. Subsequently cells were washed in three longer washing steps of 5 to 10 minutes each and covered with PBS. The morphology of the stained cells was imaged at 10x magnification with a Zeiss Axio Scope A1 microscope.

2.5. Cellular image analysis

Images were analyzed with a self-written MATLAB routine for edge detection. Only objects with a higher brightness than the manually set threshold and an area above 350 μm^2 were recognized as cells. Holes in the objects were filled automatically and touching objects were separated. From the determined area *A* and the circumference *p,* the dimensionless shape factor σ was calculated.

$$\sigma = 4\,\pi\,\frac{A}{p^2} \tag{1}$$

The shape factor describes the shape of the object and provides information about the cell morphology. A value of 1 describes a perfect circular shape, whereas values tending to 0 correspond to a completely irregular shape. 150 to 400 cells were analyzed per treatment method.

2.6. Statistics

Values that differed by $p<0.05$ were regarded as statistically significant, as evaluated using independent, two-sample t-tests for unequal sample sizes.

3. Results

3.1. Surface patterning

3.1.1. Pattern analysis

The transfer quality and pattern stability under physiological conditions were evaluated by measuring the groove width and depth of unirradiated and irradiated gelatin samples in comparison with the templates. Shown in Figure 2, the surfaces flatness of the freshly prepared unirradiated (b) and irradiated gelatin (c) were similar to the template (a). The storage in physiological conditions resulted in increasing surface waviness with conical indentations (Figure 2 (d) and (e)).

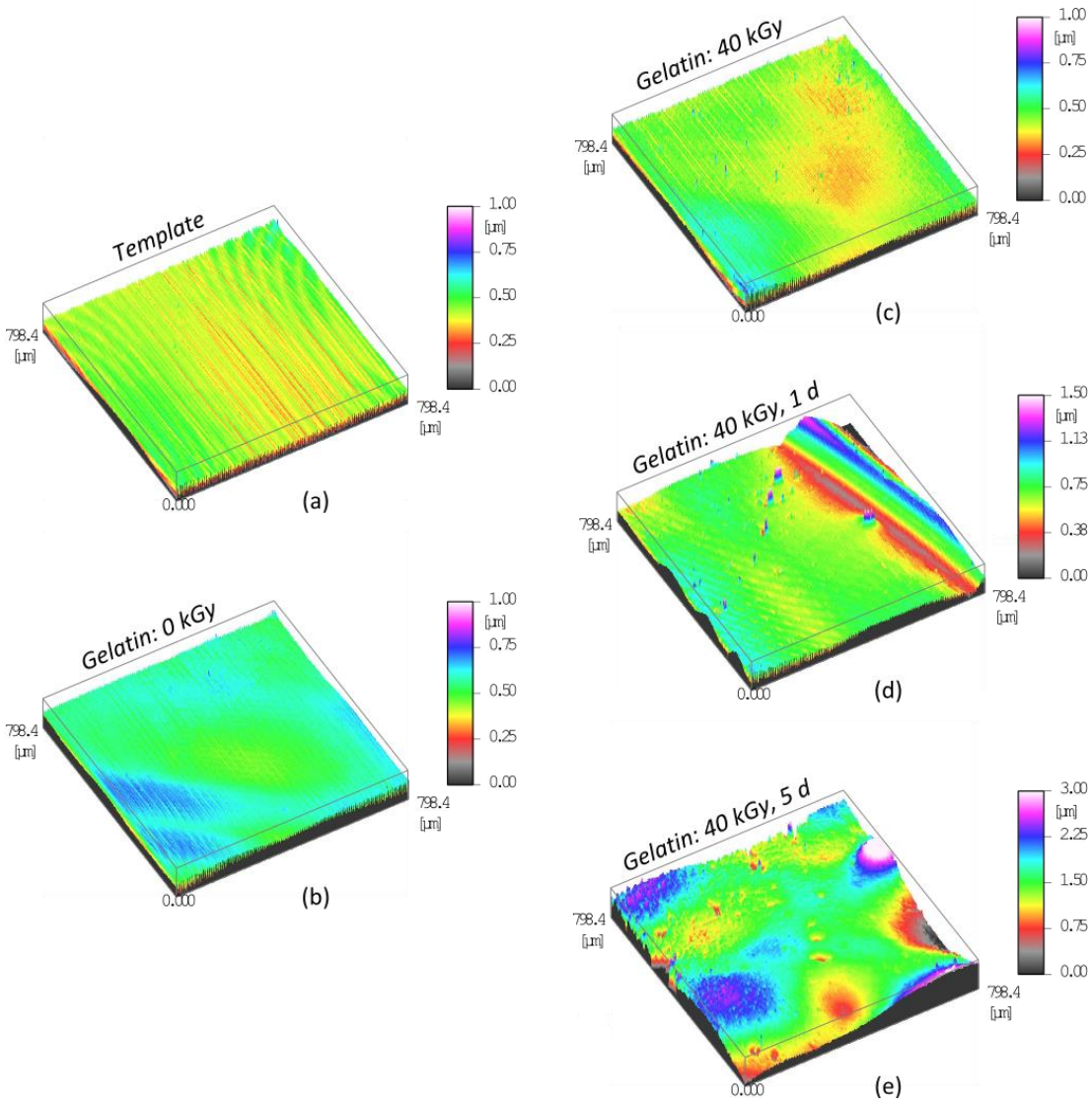

Figure 2 3D spectral illustration of 798.4 µm x 798.4 µm surface area of the template and the gelatin samples with 3.5 µm wide grooves. The profile of the gelatin is inverted. The irradiated gelatin was measured over a period of 5 days with storage in HBSS solution with 1% penicillin-streptomycin at 37 °C.

In Figure 3, the groove widths of the freshly produced samples were nearly identical to those of the template, differing less than 10 %. However, this percent difference generally decreased to less than 0.5 % as the template width increased, suggesting improved pattern transfer of the wider structures. Statistically significant differences in the widths are indicated in Figure 3 with an asterisk. The grooves of the irradiated and unirradiated gels were generally equivalent directly after fabrication, with the unirradiated grooves slightly thinner in one instance.

A time-independent decline of the average groove width in physiological conditions was visible for most grooves in comparison with the 40 kGy gels directly after synthesis, with the exception of the 17 µm structures. Generally, wider grooves had the greatest absolute decline, with respective declines from 0.63 µm up to 12.2 µm for the narrowest to widest grooves. The declines amounted to less than 10 % the original widths, excluding the larger decline of 16 % initially observed in the smallest 3.75 µm structures and the outlying increase in the width of the 17 µm structures after 5 days in physiological conditions.

Furthermore, the storage in physiological conditions affected the overall hydrogel shape and correspondingly led to a significant increase in the standard deviation of the groove widths. Changes to the overall sample surfaces were quantified by the waviness, which increased from 0.2 µm for the template up to a maximum of 0.9 µm for the gelatin hydrogels after 5 days in physiological conditions. See supplementary Figure S7 for details.

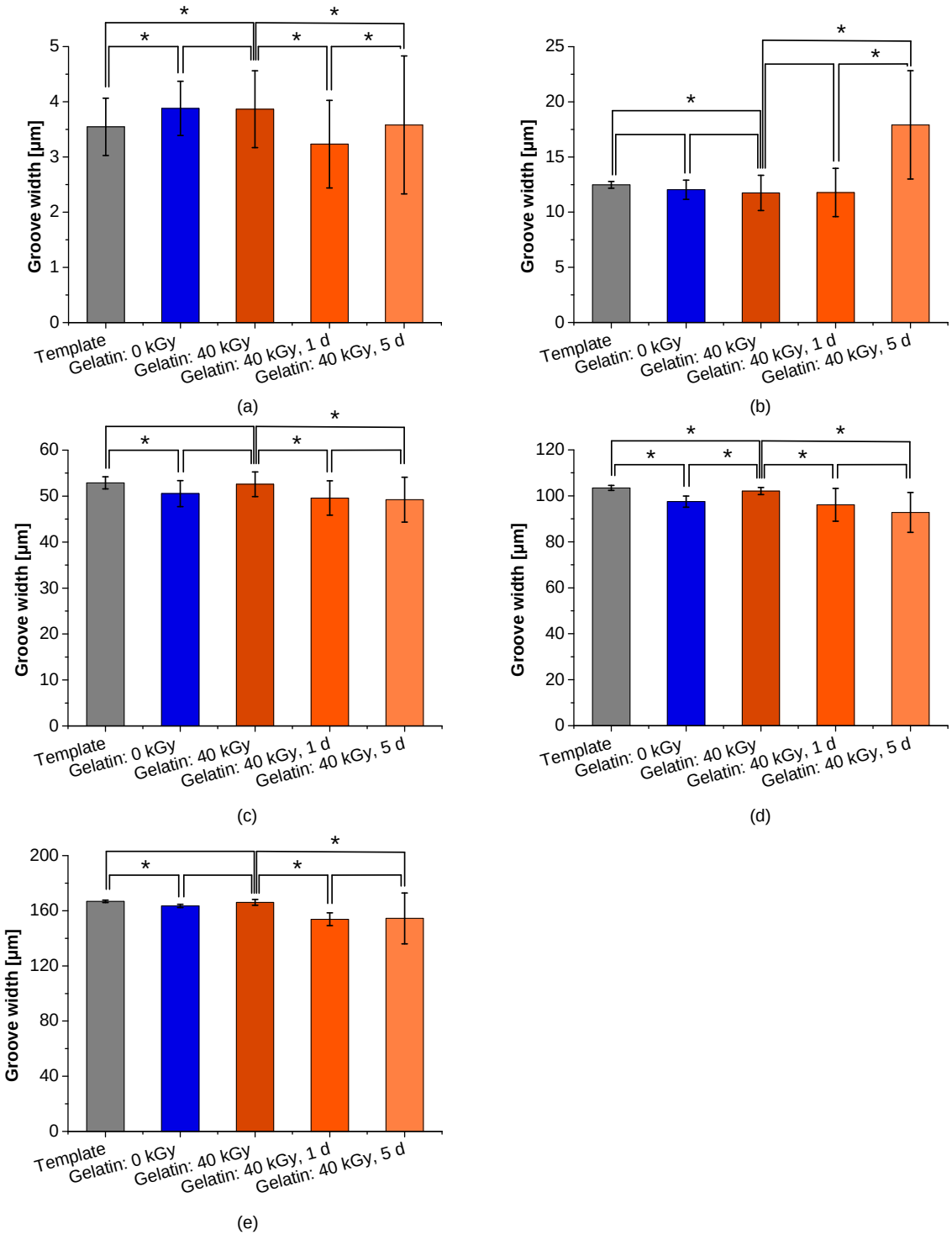

Figure 3 Groove widths for the templates (gray), unirradiated gelatin samples (blue) and irradiated samples (orange) for template groove widths of (a) 3.75 µm, (b) 17 µm, (c) 50 µm, (d) 96 µm and (e) 170 µm. The values of the gelatin samples were determined from inverted and polynomial fitted raw data. Widths were compared for the template, 0 kGy and 40 kGy structures directly after fabrication, while comparisons were also made on the 40 kGy samples after fabrication and up to 5 days storage in physiological conditions. Significant differences ($p<0.05$) in the widths are indicated with an *. Error bars represent the standard deviation.

Most of the above observed phenomena also occurred for the groove heights, as shown in Figure 4, however the general reproducibility of the overall template depth was much lower. Given that one template consisted of a mix of repeating 17 to 170 µm structures, the height of these mixed grooves could not be quantified individually with respect to the individual widths. Therefore, comparisons are made between the structures obtained from the smallest 3.75 µm grooves or the mixed-grooves template.

In contrast to the widths, the depths of the structures differed strongly from the templates. As shown in Figure 4 (a), the average depth of the 3.75 µm grooves on the unirradiated samples was only 31 % of the original template depth, while an irradiation dose of 40 kGy improved the template transfer to 43 % the original depth. In Figure 4 (b), the mixed groove template produced structures that were 47 % of the original depth for the unirradiated gels, which increased to 57 % for the irradiated samples. Overall, the depth of the transferred structures compared to the templates was improved for the larger, mixed-groove template and 40 kGy irradiated samples.

Similar to the widths in physiological conditions, the depth of the irradiated samples generally decreased, while the standard deviation increased. This decrease in groove depth was not clearly associated with the length of time spent in physiological conditions, as the smaller grooves only displayed significant differences after 5 days, while the larger mixed-grooves were reduced after 1 day and then remained constant after 5 days incubation.

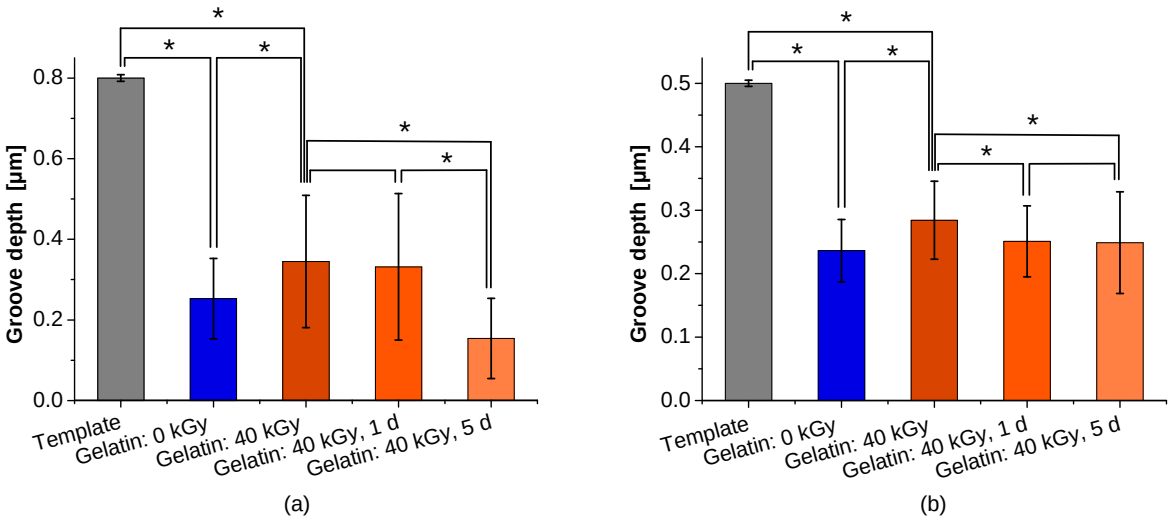

Figure 4 Average grooves depths on the unirradiated gelatin samples (blue) and irradiated samples (orange), prepared from templates with (a) 3.75 µm grooves and (b) the larger, mixed grooves. For comparison, the depths of the template grooves (gray) were determined by atomic force microscopy. The hydrogel samples were analyzed by 3D confocal microscopy from inverted and polynomial fitted data. Depths were compared for the template, 0 kGy and 40 kGy structures directly after fabrication, while comparisons were also made on the 40 kGy samples after fabrication and up to 5 days storage in physiological conditions. Significant differences ($p<0.05$) in the widths are indicated with an *. Error bars represent the standard deviation.

3.1.2. Cell morphology related to surface topography

A detailed analysis of the cell morphology in response to the surface topography was performed using immunostaining of NIH 3T3 fibroblast cells together with fluorescence microscopy followed by image evaluation. On samples prepared in contact with the smooth, unstructured aluminum plate, cells adhered undirected and mainly exhibited a three-pointed star shape, as shown in the left column of Figure **5**. This shape led to a larger cell area (on average 1094 µm^2; 1 d) and smaller shape factor (on average 0.12; 1 d), as given in Figure 6. The cells on the 3.75 µm template-structured gels orientated primarily along the grooves and exhibited a more elongated shape (Figure **5**, right column). The average shape factor was 0.15 (1 d) with an average cell area of 879 µm^2 (1 d). These trends were consistently observed after 1 and 4 days of culture, as can be seen in Figure 6.

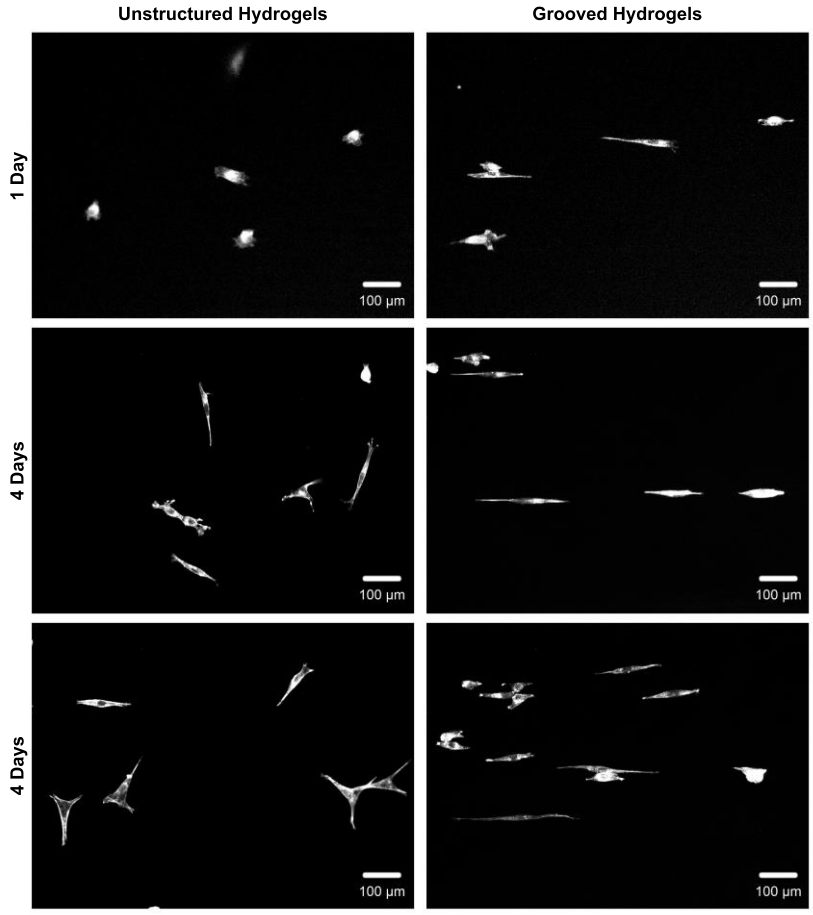

Figure 5 10x magnified images of fibroblasts on irradiated 10 wt% gelatin samples with inverted topography of (left column) an unstructured, smooth aluminum plate and (right column) a template with 3.75 µm grooves, with images taken after 1 and 4 days of culture.

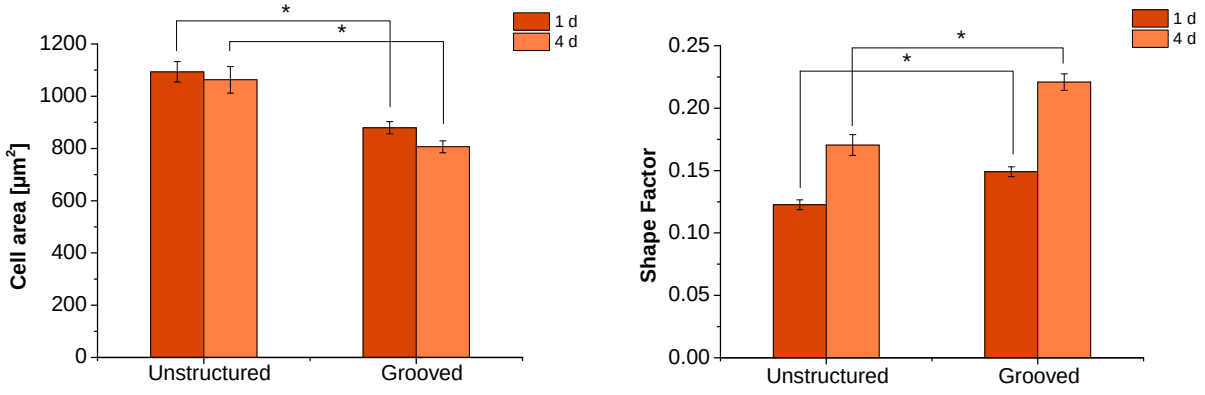

Figure 6 (a) Average cell area and (b) average shape factor of cultured fibroblasts on irradiated 10 wt% gelatin samples with unstructured and 3.75 µm grooved topographies after one and four days cultivation. The error bars represent the standard error of the mean. Statistical significance (*) indicates $p<0.05$.

4. Discussion

In exploring the functionalization of hydrogels for applications in tissue engineering and biomedicine, topographical modification can have a significant influence on cellular morphology, adhesion and proliferation. Using irradiation-induced crosslinking, a simple and effective micropatterning method to produce structured gelatin hydrogels was developed.

Once the templates were fabricated, electron irradiation crosslinking lead to easily reproducible, structured hydrogels that were stable in ambient and physiological conditions. In comparison with the preparation of unstructured radiation-crosslinked gelatin, only one additional step of preheating the template was performed. This technique therefore has a significant advantage over time-consuming techniques such as 3D cell assembling (Billiet et al. 2012), rapid prototyping robotic dispensing (Ang et al. 2002), two photon-polymerization (Liska et al. 2007) or direct ink writing (Geng et al. 2005), which all require precise control over the material properties during synthesis. In the present method, sample detachment from the template after irradiation was fast and led to no major deformation of the surface structure. Larger-scale sample deformations that were observed under physiological conditions could be explained by the swelling in HBSS solution, potentially resulting in random denting of the sample surface. Wisotzki et al. (2014) showed that a temperature increase causes a loss of liquid and therefore a change in the hydrogel volume. It is also possible that shape deviations and indentations were caused by the N_2 stream when removing the HBSS residues.

In terms of pattern transfer, the effectiveness of this preparation method was demonstrated by the similarity in the groove widths (within 10 %) obtained from the samples directly after crosslinking in comparison with the original templates. The widths of the unirradiated hydrogels were comparable to or slightly smaller than the irradiated, indicating that some of the unirradiated gelatin potentially remained on the template after detaching from the substrate. Alternatively, the process of filling the template could be hindered by the viscosity of the gelatin, resulting in reduced groove dimensions. The irradiated samples were stiffer and typically exhibited improved detachment and pattern transfer, potentially as a result of the increased stability of the crosslinked structure. Previously, macroscopic shrinking of the hydrogels during

irradiation of over 15 % the original sample weight and dimensions was observed at this dose and concentration (Wisotzki et al. 2014). Interestingly, this shrinking effect did not appear to influence the pattern transfer on a microscopic level, given the similarity in the widths obtained from the templates and irradiated structures. Perhaps surface tension between the template and hydrogel interface played a role in maintaining the size of the structures during crosslinking.

In physiological conditions, the grooves exhibited a high level of stability. While a general reduction in the groove widths was observed for the samples after exposure physiological conditions, the standard deviation also increased. Significant changes to the groove widths were typically observed after one day, but remained consistent after 5 days in physiological conditions. It is possible that temperature-dependent fluid loss and aging could reduce the hydrogel volume and thus the groove widths, as water sorption of gelatin is reduced at higher temperatures. However, a macroscopic reduction in the swelling ratio of around 30 % obtained in physiological versus ambient conditions (Wisotzki et al. 2014) was not observed to this extent in the microstructures. Water loss could also lead to increased brittleness and fragility of the microstructures, potentially explaining the proportionately larger deviation observed in the structure dimensions. In two instances, the groove width increased in physiological conditions. This irregular increase could have been caused by local swelling, as competing swelling and thermal degradation processes occur simultaneously. Nevertheless, the structures remained highly stable after crosslinking over the 5 day experimental period. This high resolution down to several micrometers is comparable to or better than many laser-based, nozzle-based and printer-based microfabrication techniques (Billiet et al. 2012).

The large differences between the groove depths on the hydrogels and templates were probably related to the high depth-to-width ratio of the grooves. The 3.75 µm grooves were particularly deep and narrow, thus the poured gelatin could have solidified before it reached the bottom of the template when preparing the samples. As previously mentioned, the influence of the viscosity and flow of the gel solution could have also hindered filling the templates completely. Pattern transfer could be investigated using a range of gelatin concentrations to study this possible effect. A further problem could have arisen upon detachment. The resulting structures were fragile and subjected to high frictional forces, which could lead to a portion of the gelatin sticking to the

template during the detachment process. This effect would explain the large standard deviations, which were proportionately twice as large as those obtained for the widths. The irradiated samples had deeper grooves on average than those on the unirradiated gels, again suggesting that increased stiffness from irradiation crosslinking improved the removal of the template and subsequent pattern transfer, particular when considering the depth profiles.

Though the depth of the hydrogel structures differed significantly from the template, the grooves were sufficiently pronounced enough to induce an elongated shape in the seeded fibroblasts along the direction of the structures. This cell behavior was expected since it is well established that many cell lines display contact guidance on grooved substrates (Clark et al. 1991; den Braber et al. 1995; den Braber et al. 1996b; den Braber et al. 1996a, 1998; Flemming et al. 1999; Matsuzaka et al. 2000; van Kooten et al. 1998; Walboomers et al. 1999; Walboomers et al. 2001; Wójciak-Stothard 1995; Wójciak-Stothard et al. 1995). On the gelatin hydrogels imprinted by smooth aluminum plates, the fibroblasts did not display a preferred orientation because of the unstructured topography (Teixeira et al. 2003, Wisotzki et al. 2016). In contrast, an elongated cell shape was observed on the structured samples. This cell shape corresponded to a smaller average cell area and larger shape factor when compared to the cells grown on unstructured gelatin. Since contact guidance promotes growth along the axis of the grooves, it is logical that the average cell area could be reduced with respect to unrestricted cells. Similarly, the overall branching of the cells could decrease from this restriction, as elongation was promoted in only one dimension. As a result, a larger shape factor was observed. Interestingly, these trends were still observed after 4 days in physiological conditions, providing further indication that the patterned structures survived and continued to influence cell growth during the experimental period. Since the grooves were much smaller than the cell diameter, the cells must have spanned several grooves, as already demonstrated by other studies in which micrometer grooved substrates were employed (den Braber et al. 1996b; Clark et al. 1990; Karuri et al. 2008; Oakley et al. 1997; Uttayarat et al. 2005; Walboomers et al. 1999). Teixeira et al. (2003) also showed that cells were able to adhere to the bottom of the grooves of 2.1 µm width and 150 nm depth, which results in a depth-to-width ratio comparable to the employed gelatin grooves.

These results are significant considering that many studies have shown that the adhesion of various cell types increases for a certain range of surface roughness and may even require a minimum degree of roughness for adhesion (Deligianni et al. 2000; Hallab et al. 2001; Eisenbarth et al. 1996; Ranella et al. 2010). On the microscopic scale, such structures serve as potential adhesion points for the cells and could be tuned for specific applications. Overall, pre-synthesized templates were successfully used to pattern gelatin hydrogels in combination with high energy radiation crosslinking in order to create stable hydrogels that promoted and directed cellular growth. Furthermore, the impressive resolution of several to hundreds of micrometers introduces the possibility to pattern a wide range of structures on scales that are highly relevant to cellular growth.

5. Conclusion and outlook

The patterning of a substrate surface is a common method to influence cell morphology. Often incorporated patterns consist of groove structures on which the cells form elongated morphologies by contact guidance. This developed method allowed for quick and easy patterning of hydrogels with a range of structures from 3.75 to 170 µm. Electron Irradiation led to additional crosslinking of the structures, exhibiting relatively stable groove widths during the detachment process as well as under physiological conditions. In particular, the widths of 3.75 µm grooves, which are highly interesting for cellular applications, varied by less than 1 µm. The pattern transfer of the groove depths was less accurate, probably limited by the depth to width ratio and flow effects from the gelatin viscosity during the filling of the template. Deeper grooves could be achieved by increased preheating of the template, a lower concentration of gelatin corresponding to a reduced viscosity or even a higher irradiation dose to improve detachment. An anti-adhesive biocompatible layer on the template could also potentially reduce the gelatin losses during the detachment process.

Cell experiments confirmed that the hydrogel structures survived in physiological conditions, while the topography had an essential influence on cell morphology and adhesion. Fibroblasts displayed an elongated morphology on the grooved samples consistently after 1 and 4 days, in

comparison with the larger cell areas and random morphologies observed on the unstructured gels.

Overall, this easy-to-reproduce method demonstrated comprehensive microstructuring of gelatin hydrogel surfaces and exhibited a direct influence on cellular processes. Due to the simple methodology, a large number of different patterns could potentially be produced and utilized to influence cellular growth. By controlling the roughness of the template, adhesion could be further tuned and adapted, which is a crucial factor in the development of an anti-adhesive cell carrier. As a result, electron irradiated gelatin in combination with prestructured templates is a promising and versatile technique to synthesis patterned hydrogels with a wide range of biomedical applications. This methodology could be transferred to other biopolymers that are responsive to reagent-free high energy irradiation crosslinking, such as collagen, to further increase the impact of this process in the synthesis of biomedical materials for application in the field of tissue engineering.

Acknowledgements

The authors gratefully acknowledge Dr. W. Knolle and R. Konieczny for electron irradiation, I. Herold and T. Liebeskind for lithographic production and cleaning of the silicon templates, A. Bischoff for AFM measurement and Dr. G. Böhm for assisting with 3D confocal microscopy. Funding was provided in parts by the German Research Foundation (DFG) via the Priority Program SPP 1681 and the DFG project BIOSTRAIN. E.I. Wisotzki also acknowledges funding by the Natural Sciences and Engineering Research Council of Canada (NSERC) via a PGS D.

References

Ang T, Sultana F, Hutmacher D, Wong Y, Fuh J, Mo X, Loh H, Burdet E, Teoh S (2002) Fabrication of 3D chitosan–hydroxyapatite scaffolds using a robotic dispensing system. Materials Science and Engineering: C 20:35–42.

Biela SA, Su Y, Spatz JP, Kemkemer R (2009) Different sensitivity of human endothelial cells, smooth muscle cells and fibroblasts to topography in the nano–micro range. Acta Biomaterialia 5:2460–2466.

Billiet T, Vandenhaute M, Schelfhout J, van Vlierberghe S, Dubruel P (2012) A review of trends and limitations in hydrogel-rapid prototyping for tissue engineering. Biomaterials 33:6020–6041

Chou L, Firth JD, Uitto VJ, Brunette DM (1995) Substratum surface topography alters cell shape and regulates fibronectin mRNA level, mRNA stability, secretion and assembly in human fibroblasts. J Cell Sci 108:1563–1573.

Clark P, Connolly P, Curtis AS, Dow JA, Wilkinson CD (1991) Cell guidance by ultrafine topography in vitro. J. Cell Sci. 99:73-77.

Clark P, Connolly P, Curtis AS, Dow JA, Wilkinson CD (1990) Topographical control of cell behaviour. 2. Multiple grooved substrata. Developmental Cell 108:635–644

Deligianni DD, Katsala ND, Koutsoukos PG, Missirlis YF (2000) Effect of surface roughness of hydroxyapatite on human bone marrow cell adhesion, proliferation, differentiation and detachment strength. Biomaterials 22:87–96.

den Braber ET, de Ruijter JE, Ginsel LA, von Recum AF, Jansen JA (1996a) Quantitative analysis of fibroblast morphology on microgrooved surfaces with various groove and ridge dimensions. Biomaterials 17:2037–2044.

den Braber ET, de Ruijter JE, Ginsel LA, von Recum AF, Jansen JA (1998) Orientation of ECM protein deposition, fibroblast cytoskeleton, and attachment complex components on silicone microgrooved surfaces. J. Biomed. Mater. Res. 40:291–300.

den Braber ET, de Ruijter JE, Smits HT, Ginsel LA, von Recum AF, Jansen JA (1996b) Quantitative analysis of cell proliferation and orientation on substrata with uniform parallel surface micro-grooves. Biomaterials 17:1093–1099.

den Braber ET, de Ruijter JE, Smits HTJ, Ginsel LA, von Recum AF, Jansen JA (1995) Effect of parallel surface microgrooves and surface energy on cell growth. J. Biomed. Mater. Res. 29:511–518.

Dent EW, Gertler FB (2003) Cytoskeletal Dynamics and Transport in Growth Cone Motility and Axon Guidance. Neuron 40:209–227.

Dunn GA, Brown AF (1986) Alignment of fibroblasts on grooved surfaces described by a simple geometric transformation. J Cell Sci 83:313–340.

Eisenbarth E, Meyle J, Nachtigall W, Breme J (1996) Influence of the surface structure of titanium materials on the adhesion of fibroblasts. Biomaterials 17:1399–1403.

El-Sherbiny IM, Yacoub MH (2013) Hydrogel scaffolds for tissue engineering: Progress and challenges. Global Cardiology Science and Practice 2013:38.

Flemming R, Murphy C, Abrams G, Goodman S, Nealey P (1999) Effects of synthetic micro- and nano-structured surfaces on cell behavior. Biomaterials 20:573–588.

Friedl P (2004) Prespecification and plasticity: shifting mechanisms of cell migration. Current Opinion in Cell Biology 16:14–23.

Fukuda J, Khademhosseini A, Yeo Y, Yang X, Yeh J, Eng G, Blumling J, Wang C, Kohane DS, Langer R (2006) Micromolding of photocrosslinkable chitosan hydrogel for spheroid microarray and co-cultures. Biomaterials 27:5259–5267.

Geng L, Feng W, Hutmacher DW, San Wong Y, Tong Loh H, Fuh JY (2005) Direct writing of chitosan scaffolds using a robotic system. Rapid Prototyping Journal 11:90–97.

Haga H, Irahara C, Kobayashi R, Nakagaki T, Kawabata K (2005) Collective Movement of Epithelial Cells on a Collagen Gel Substrate. Biophysical Journal 88:2250–2256.

Hallab NJ, Bundy KJ, O'Connor K, Moses RL, Jacobs JJ (2001) Evaluation of Metallic and Polymeric Biomaterial Surface Energy and Surface Roughness Characteristics for Directed Cell Adhesion. Tissue Engineering 7:55–71.

Hynes RO (2009) The Extracellular Matrix: Not Just Pretty Fibrils. Science 326:1216–1219.

Karuri NW, Nealey PF, Murphy CJ, Albrecht RM (2008) Structural organization of the cytoskeleton in SV40 human corneal epithelial cells cultured on nano- and microscale grooves. Scanning 30:405–413

Khademhosseini A, Eng G, Yeh J, Fukuda J, Blumling J, Langer R, Burdick JA (2006) Micromolding of photocrosslinkable hyaluronic acid for cell encapsulation and entrapment. J. Biomed. Mater. Res. 79:522–532.

Khademhosseini A, Langer R (2007) Microengineered hydrogels for tissue engineering. Biomaterials 28:5087–5092.

Langer R, Vacanti J (1993) Tissue engineering. Science 260:920–926.

Liska R, Schuster M, Inführ R, Turecek C, Fritscher C, Seidl B, Schmidt V, Kuna L, Haase A, Varga F, Lichtenegger H, Stampfl J (2007) Photopolymers for rapid prototyping. J Coat Technol Res 4:505–510.

Luca AC de, Zink M, Weidt A, Mayr SG, Markaki AE (2015) Effect of microgrooved surface topography on osteoblast maturation and protein adsorption. J. Biomed. Mater. Res. 103:2689–2700

Ma PX (2004) Scaffolds for tissue fabrication. Materials Today 7:30–40.

Ma PX (2005) Tissue engineering. In: Kroschwitz J (ed) Encyclopedia of Polymer Science and Technology, 3rd edn. John Wiley & Sons Inc., Hoboken, NJ, 261–291.

Ma PX (2008) Biomimetic materials for tissue engineering. Advanced Drug Delivery Reviews 60:184–198.

Matsuzaka K, Walboomers F, Ruijter A, Jansen JA (2000) Effect of microgrooved poly-l-lactic (PLA) surfaces on proliferation, cytoskeletal organization, and mineralized matrix formation of rat bone marrow cells. Clinical Oral Implants Research 11:325–333.

Meyle J, Gültig K, Nisch W (1995) Variation in contact guidance by human cells on a microstructured surface. J. Biomed. Mater. Res. 29:81–88.

Nikkhah M, Edalat F, Manoucheri S, Khademhosseini A (2012) Engineering microscale topographies to control the cell–substrate interface. Biomaterials 33:5230–5246.

Oakley C, Jaeger NA, Brunette DM (1997) Sensitivity of Fibroblasts and Their Cytoskeletons to Substratum Topographies: Topographic Guidance and Topographic Compensation by Micromachined Grooves of Different Dimensions. Experimental Cell Research 234:413–424

Prasad Chennazhy K, Krishnan LK (2005) Effect of passage number and matrix characteristics on differentiation of endothelial cells cultured for tissue engineering. Biomaterials 26:5658–5667.

Ranella A, Barberoglou M, Bakogianni S, Fotakis C, Stratakis E (2010) Tuning cell adhesion by controlling the roughness and wettability of 3D micro/nano silicon structures. Acta Biomaterialia 6:2711–2720.

Revi D, Geetha C, Thekkuveettil A, Anilkumar TV (2016) Fibroblast-loaded cholecyst-derived scaffold induces faster healing of full thickness burn wound in rabbit. Journal of Biomaterials Applications 30:1036–1048

Rørth P (2011) Whence Directionality: Guidance Mechanisms in Solitary and Collective Cell Migration. Developmental Cell 20:9–18.

Sefton MV, Gemmell CH, Gorbet MB (2012) Chapter II.5.2 – Nonthrombogenic Treatments and Strategies. In: Biomaterials Science. Elsevier, 1488–1509.

Stevens MM (2005) Exploring and Engineering the Cell Surface Interface. Science 310:1135–1138.

Teixeira AI, Abrams GA, Bertics PJ, Murphy CJ, Nealey, PF (2003) Epithelial contact guidance on well-defined micro- and nanostructured substrates. Journal of Cell Science 116:1881–1892.

Uttayarat P, Toworfe GK, Dietrich F, Lelkes PI, Composto RJ (2005) Topographic guidance of endothelial cells on silicone surfaces with micro- to nanogrooves: Orientation of actin filaments and focal adhesions. J. Biomed. Mater. Res. 75:668–680.

van Kooten TG, Whitesides JF, Recum AF von (1998) Influence of silicone (PDMS) surface texture on human skin fibroblast proliferation as determined by cell cycle analysis. J. Biomed. Mater. Res. 43:1–14.

Walboomers X, Croes H, Ginsel L, Jansen J (1999) Contact guidance of rat fibroblasts on various implant materials. J. Biomed. Mater. Res. 47:204–212.

Walboomers XF, Monaghan W, Curtis ASG, Jansen JA (2001) Attachment of fibroblasts on smooth and microgrooved polystyrene. J. Biomed. Mater. Res. 55:669.

Weibel DB, DiLuzio WR, Whitesides GM (2007) Microfabrication meets microbiology. Nat Rev Micro 5:209–218.

Wisotzki EI, Hennes M, Schuldt C, Engert F, Knolle W, Decker U, Käs JA, Zink M, Mayr SG (2014) Tailoring the material properties of gelatin hydrogels by high energy electron irradiation. J. Mater. Chem. B 2:4297–4309.

Wisotzki EI, Friedrich RP, Weidt A, Alexiou C, Mayr SG, Zink M (2016) Cellular Response to Reagent-Free Electron- Irradiated Gelatin Hydrogels. Macromol. Biosci. 16:914-924.

Wójciak-Stothard B (1995) Activation of macrophage-like cells by multiple grooved substrata. Topographical control of cell behaviour. Cell Biology International 19:485–490.

Wójciak-Stothard B, Curtis ASG, McGrath M, Sommer I, Wilkinson CDW, Monaghan W (1995) Role of the cytoskeleton in the reaction of fibroblasts to multiple grooved substrata. Cell Motil. Cytoskeleton 31:147–158.

Wolf K (2003) Amoeboid shape change and contact guidance: T-lymphocyte crawling through fibrill ar collagen is independent of matrix remodeling by MMPs and other proteases. Blood 102:3262–3269.

Wood A (1998) Contact guidance on microfabricated substrata: the response of teleost fin mesenchyme cells to repeating topographical patterns. J Cell Sci 90:667–681.

Yeh J, Ling Y, Karp JM, Gantz J, Chandawarkar A, Eng G, Blumling III J, Langer R, Khademhosseini A (2006) Micromolding of shape-controlled, harvestable cell-laden hydrogels. Biomaterials 27:5391–5398.